sustainability

MDPI

Article

Cotton Spinning Waste as a Microporous Activated Carbon: Application to Remove Sulfur Compounds in a Tunisian Refinery Company

Bechir Wannassi [1], Mohammad Kanan [2,*], Ichrak Ben Hariz [3], Ramiz Assaf [4], Zaher Abusaq [2], Mohamed Ben Hassen [1], Salem Aljazzar [2], Siraj Zahran [2], Mohammed T. Khouj [2] and Ahmad S. Barham [5]

[1] Textile Laboratory Engineering 'LGTex', University of Monastir, Ksar Hellal, Monastir 5078, Tunisia
[2] Jeddah College of Engineering, University of Business and Technology, Jeddah 21448, Saudi Arabia
[3] Tunisian Society of Refinery Industries, Bizerte 7021, Tunisia
[4] Industrial Engineering Department, An-Najah National University, Nablus 00970, Palestine
[5] Department of Chemistry, The University of Jordan, Amman 11942, Jordan
* Correspondence: m.kanan@ubt.edu.sa

Abstract: The petroleum industry plays a vital role in the economies of developing countries. Refinery wastewater pollution has increased in recent years due to the increase in the industrial and urban use of petroleum products. The present work demonstrates how textile waste can be modified into a material that can effectively remove sulfur pollutants from refinery wastewater. An economic activated carbon (AC) material was developed by using cotton spinning waste from a textile company. The chemical activation was carried out using nitric acid (HNO_3), hydrogen peroxide (H_2O_2), and potassium hydroxide (KOH). The characterization of the obtained activated carbons was performed using the SEM, BET, and FTIR techniques. The effect of the experimental adsorption condition was investigated using both bed and batch isotherms. The results show that effluent flow has the highest effect on sulfur compound adsorption. The greatest adsorption capacity of the sulfur compounds was found to be around 168.4 mg·g^{-1}. The equilibrium data were investigated using the Freundlich, Langmuir, Dubinin–Radushkevich, Tóth, and Sips isotherm models. The Langmuir model exhibited the best fit (R^2 = 0.98) for the sulfur compounds' adsorption, which implies that their adsorption onto the synthesized AC was homogeneous. The kinetic data were tested with pseudo-first-order, pseudo-second-order, and intraparticular diffusion equations. The pseudo-second-order equation described the kinetic data well (R^2 = 0.99), indicating that this adsorption may be restricted by the chemisorption process. These properties under optimal conditions make the obtained ACs suitable for use in refinery wastewater treatment.

Keywords: cotton waste; activated carbon; kinetic study; bed adsorption; chemical activation; removal; refinery wastewater

Citation: Wannassi, B.; Kanan, M.; Hariz, I.B.; Assaf, R.; Abusaq, Z.; Ben Hassen, M.; Aljazzar, S.; Zahran, S.; Khouj, M.T.; Barham, A.S. Cotton Spinning Waste as a Microporous Activated Carbon: Application to Remove Sulfur Compounds in a Tunisian Refinery Company. *Sustainability* **2023**, *15*, 654. https://doi.org/10.3390/su15010654

Academic Editors: Gassan Hodaifa, Mounia Achak, Khaoula Khaless and Edvina Lamy

Received: 18 November 2022
Revised: 16 December 2022
Accepted: 27 December 2022
Published: 30 December 2022

1. Introduction

Environmental pollution has increased in recent years with the increase in industrial and urban development. The petroleum industry plays a vital role in the economies of developing countries across the world. Oil refining is an essential operation during petroleum processing, and it uses a huge quantity of chemical products and generates both solid waste and wastewater [1], which are considered hazardous waste. In fact, refinery wastewater has high quantities of heavy metals (more than 50 mg·dm^{-3}), phenols (more than 150 mg·dm^{-3}), benzene (more than 75 mg·dm^{-3}), and Chemical Oxygen Demand (COD) (between 280 and 1100 mg·dm^{-3}) [2–6].

The removal of hazardous components is a requirement before the discharge of this type of wastewater and before its reuse [7,8]. Therefore, treating effluent is required in

order to eliminate hazardous contaminants [9]. Several methods have been investigated for the treatment of refinery wastewater, including physical, chemical, and biological methods.

A membrane bioreactor has been successfully used to remove pollutants from petroleum industry wastewater. Rahman et al. evaluated the use of a cross-flow membrane bioreactor for the treatment of refinery wastewater. Their results showed that this technique can remove more than 93% of COD from refinery effluents and that its efficiency does not depend on the hydraulic retention time [10]. Razavi et al. studied the use of a hollow-fiber membrane bioreactor to treat refinery wastewater. The effects of flux, temperature, and hydraulic retention parameters were evaluated. According to the findings of this investigation, COD elimination can reach 82% [11]. However, this method comes with several specific precautions. Membrane fouling is a major problem that can frequently occur. Moreover, this seriously affects the quality of the reclaimed water and the efficiency of the membrane. However, its use was only recently tested in a pilot test [12–14].

Yan et al. [15] investigated the use of electrochemical processes in the treatment of petroleum refinery wastewater. These processes introduce air and a few particles of iron into classical two-dimensional reactors. In optimal experimental conditions, the salinity and COD removal efficiency were 84 $\mu S\ cm^{-1}$ and 92.8%, respectively. However, the use of the electrochemical method is limited for organic material removal [16,17]. Its higher cost and lower efficiency also limit its industrial application [18–20].

The microbiological treatment of industrial refinery wastewater has also been investigated using several types of microorganisms [21,22]. This method has been used to oxidize organic matter existing in refinery effluent into simple products, such as CH_4, H_2O, and CO_2, under aerobic, anaerobic, and semi-aerobic conditions [23,24]. Ebrahimi et al. investigated the use of this kind of treatment in an experimental pilot plant. He demonstrated, in suitable experimental conditions, a COD removal efficiency of around 78% and a biomass production of 1420 g daily [25]. Hayat et al. carried out an investigation of a microbiological approach to treat refinery wastewater. The interaction between metals and the functional groups of microorganisms was analyzed. The quantitative results revealed that the bacteria had developed a new level of metal resistance [22]. However, firstly, the use of a biological approach for refinery effluent treatment can cause serious problems due to the excessive production of sludge [26]. Secondly, these methods generate diverse operational problems, such as the generation of residual sludge and toxic gases, the partial elimination of refractory compounds, and the need for a large land area.

Many researchers have successfully used the adsorption approach to treat refinery wastewater [27–31]. The selection of this method is based on its high potential to remove toxic compounds and its cost-effective nature. El-Naas evaluated the use of activated carbon using local material prepared from date pits as a precursor in the treatment of refinery wastewater. Several kinetic and isotherm models were tested with batch adsorption. The Sips isotherm was proved to be the best model to describe the equilibrium isotherm, whereas the pseudo-second-order model gave the best fit for the kinetics data. More than 85% regeneration efficiency was found after four cycles of regeneration [32]. Qinxuan et al. investigated the use of prepared activated carbon in the treatment of refinery wastewater. Their results showed that the activated carbon experimental conditions (the calcination time and temperature, chemical reagent concentration, and weight ratio of AC) have an important effect on the COD removal efficiency. Their results also showed that the COD efficiency increases with a decrease in the weight ratio of effluent [33]. Several researchers have used biomass as a precursor of activated carbon in the treatment of refinery wastewater. *Lagerstroemia speciosa* has been used as a precursor of activated carbon and showed potential to recover platinum from refinery wastewater [34]. Rice husk activated carbon has been successfully evaluated as an effective adsorbent of phenolic compound content in refinery wastewater using a column approach [35]. Date activated carbon has also been evaluated as an effective adsorbent that can reduce COD in refinery effluent [36–38].

The growth of the textile industry has resulted in massive amounts of solid waste. Indeed, 106 M tons of textile solid waste is produced annually worldwide [39]. This amount

increases from one year to the next due to the boom of the fashion industry [40]. Around the world, cotton is used the most. Cotton waste can be used as a low-cost lignocellulosic material [41–43].

Not only can cotton waste can be used to produce yarns and nonwovens [44–48], but it can also be used as a reinforcement for composite materials [49,50].

Some researchers have studied the possibility of transforming cotton waste into activated carbon. Zhao et al. [51] studied the production of activated carbon by using cotton woven waste. The waste was first dissolved using 80% H_3PO_4 and pre-soaked in a solution of 7.5% $(NH_4)_2HPO_4$. In the optimum conditions of 700–800 °C, 30 min of carbonization, and 30 min of activation, good adsorption results were obtained.

Sartova [52] utilized the boiling layer method to prepare AC from cotton biomass (stems and balls from cotton plants boiled at 800 to 850 °C for 8 min), and he demonstrated that the AC obtained had adsorption properties higher than those of industrial AC made from wood. Wanassi [53] employed cotton waste to produce activated carbon through carbonization using zinc chloride chemical activation. The obtained product enabled a high removal of anionic dye from textile wastewater.

Xu [54,55] optimized the production of activated magnetic carbon from textile waste yarn using $FeCl_3$. The results proved that this treatment is able to change the pyrolysis process of cotton textile waste, decrease the pyrolytic carbonization temperature, and prevent the production of volatiles. Fe_2O_3 and Fe_3O_4 resulting from $FeCl_3$ could help pore formation on the obtained activated carbon.

Most of these previous studies were conducted at the laboratory scale with no focus on a specific application. The main objective of our work, realized with the collaboration of a big refinery company in Tunisia, was to synthesize activated carbon from cotton fiber spinning waste and to use it to remove sulfur compounds from refinery wastewater. The whole process is illustrated in Figure 1.

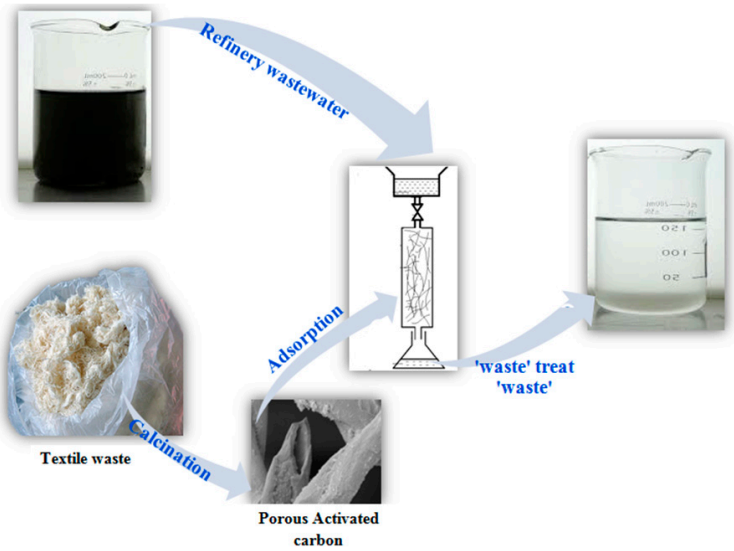

Figure 1. Process of the preparation and use of activated carbon.

2. Materials and Methods

2.1. Materials and Chemicals

The raw material used was recycled spinning cotton fiber waste obtained from Tunisian Textile Industries Company (SITEX) in Tunisia. In a previous study, we optimized the fraying process of spinning yarn waste using a mechanical machine [46]. Approximately 20% of the obtained fibers were judged to be non-reusable for another cycle of the spinning process because of their bad quality (bad mechanical properties and a high ratio of short

fibers). So, in reality, we used the waste of the waste of a low-quality and low-cost cotton fiber to produce our activated carbon (AC).

H_2O_2, KOH, and HNO_3 were purchased from Chimitex, Sousse 4000, Tunisia, Ltd. (Sousse, Tunisia). All the chemical reagents were used as received without additional treatment.

2.2. Preparation of Activated Carbon

Cotton waste fiber was washed with distilled water for the removal of impurities. Then, it was oven-dried at 85 °C until a 7–10% moisture content was obtained.

About 40 g of the dried fibers was heated to 700 °C at a heating rate of 5 °C/min in a horizontal furnace under a purified N_2 flow (10 NL/min). After the calcination process, the char was cooled under N_2 flow to room temperature. Afterward, the char was chemically activated using nitric acid (HNO_3), hydrogen peroxide (H_2O_2), and potassium hydroxide (KOH).

For HNO_3 activation, the char was impregnated with HNO_3 at a ratio of 3:1 (g HNO_3/g char). For H_2O_2 activation, 50 mL of commercial H_2O_2 solution (110 vol.; 33% *w*/*v*) was used. For KOH activation, the char was impregnated with OH solution at a ratio of 3:1 (g KOH/g char). For all samples, the reaction was kept at ambient temperature (25 °C) for 24 h. Then, the mix was dried at 85 °C for 12 h. After drying, each sample was heated to 700 °C at a heating rate of 5 °C/min in a horizontal furnace under purified N_2 flow.

After cooling down, the activated carbon (AC) was washed in hot distilled water to remove any unused activating agent and then oven-dried at 85 °C for 24 h for further utilization. The resulting ACs were denoted as HNAC, HOAC, and KAC.

2.3. Characterization Methods

Various techniques were explored to characterize the raw materials and their derived activated carbon.

2.3.1. Morphologies of ACs

The morphologies of the raw materials and their derived activated carbon were analyzed using scanning electron microscopy (FEI model Quanta 400 SEM, Philips, Andover, MA, USA).

The FEI Quanta 400 is a high-resolution field-emission scanning electron microscope. It is equipped with SE, backscatter, and energy-dispersive spectroscopy detectors, and it can operate in high vac, low vac, and Wet modes. It is also equipped with a cooling stage. The FEI Quanta 400 is an environmental SEM (ESEM). The major advantage of ESEM modes is that any material, dry non-conductive up to extreme conditions, for example, wet specimens and those containing volatile components, such as oil, can be viewed and analyzed. So, no treatment or preparation is needed to view the specimen. The magnification number is 1200.

2.3.2. Textural Characterization

HNAC, HOAC, and KAC activated carbon textural characterization were performed using N_2 adsorption isotherms at 77 K with an ASAP 2020 instrument (Micromeritics, Atlanta, GA, USA). Before the analyses, carbon was outgassed overnight under a vacuum at 623 K. The BET surface areas (SBET) of the samples were determined using N_2 adsorption isotherms in a relative pressure (P/P0) range of 0.05–0.30. The micropore surface (Smic) area and micropore volume (Vmicro) were investigated using the t-plot method. The average pore diameter (Dp) was determined according to the Density Functional Theory (DFT) method.

2.4. Fourier Transform Infrared Spectra (FTIR)

The surface chemistries of the activated carbon samples were characterized using an FTIR analysis. The samples were blended with KBr and then tabulated. The infrared

spectra of the samples were recorded using a Perkin Elmer model to detect the surface functional groups. The infrared spectra were recorded in the wave range of 600–4000 cm^{-1}.

2.5. Adsorption Experiment

2.5.1. Bed Adsorption

A schematic of the device used for the bed adsorption experiment is shown in Figure 2. Carbonized fibers (5) were packed into a glass column (4) to study their adsorption capacity. The wastewater (2) was introduced in a funnel (1) and passed through an input valve (3) to adjust the flow at 4–5.10 $m^3 \cdot h^{-1}$. First, the bed adsorption device was wetted using distilled water flowing through the column in order to improve the wetting characteristics of the activated carbon fibers. Second, the refinery wastewater sample (2) content in the funnel (1) was allowed to drain through the activated carbon bed (5) to the received reservoir (6) by gravity. Treated water was reclaimed every hour.

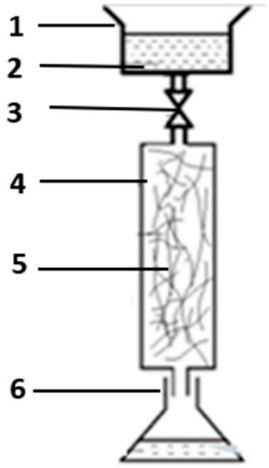

Figure 2. Bed adsorption experiment.

2.5.2. Batch Adsorption

The wastewater samples were collected from a local petroleum refinery (Tunisian Society of Refining Industry (STIR)) and preserved in dark-colored plastic containers at RT. Table 1 shows the main characteristics of the refinery wastewater.

Table 1. Refinery wastewater characteristics.

Characteristic	Value
pH	12.9
Conductivity ($ms \cdot cm^{-1}$)	126.7
Sulfide ($mg \cdot L^{-1}$)	3476
NaOH (wt%)	7.5

Batch adsorption equilibrium experiments were carried out by reacting a known amount (4.0 g) of CA with 50 mL of a real wastewater sample in a sealed glass bottle. Five samples with different initial sulfur concentrations (100, 300, 500, 800, and 1000 $mg \cdot L^{-1}$) were tested. The bottles were kept on a shaker at a constant temperature for 24 h until they reached equilibrium (final pH: 10.5).

The adsorption capacity Qt at contact time t was calculated as follows [56]:

$$Q_t = \frac{(C_0 - C_t) \cdot V}{M} \quad (1)$$

where C_t is the sulfur solution concentration at time t (mg/L), C_i is the initial sulfur concentration (mg/L) at time 0, M is the weight of the adsorbent (g), and V is the volume of the solution (L).

2.5.3. Determination of COD

The determination of COD was performed using potassium dichromate based on the American Public Health Association (APHA) standard method [57]. COD in $mg{\cdot}L^{-1}$ was calculated using the following equation:

$$COD = \frac{n{\cdot}(a - b)}{V}{\cdot}8000 \quad (2)$$

where a (mL) is the ferrous ammonium sulfate required for the titration of the blank, b (mL) is the ferrous ammonium sulfate required for the titration of the sample, n is the normality of the ferrous ammonium sulphate, and V (mL) is the sample volume.

2.6. Kinetic Models

The kinetics of the adsorption was investigated to evaluate the potential of using synthesized activated carbon as an adsorbent of sulfur compounds in refinery wastewater. In this study, several experimental conditions were explored to determine the factors that can affect the adsorption speed. The obtained experimental results were tested with three mathematical models that can describe the kinetics of interaction between synthesized activated carbon and sulfur compounds. Three of the most widely used kinetic models were investigated: pseudo-first-order, pseudo-second-order, and intra-particular diffusion models. Table 2 illustrates the mathematical forms of each model, where k_1 represents the pseudo-first-order rate constant (min^{-1}), k_2 represents the pseudo-second-order rate constant ($L{\cdot}mg^{-1}{\cdot}min^{-1}$), and k_{id} is the diffusion intraparticular constant ($mL^{-1}{\cdot}min^{-1/2}$).

Table 2. Kinetic models.

Model	Equation	Reference
Pseudo-first-order	$\log(q_e - q_t) = \log(q_e) - \frac{k_1}{2.303}\,t$	[58]
Pseudo-second-order	$\frac{t}{q_t} = \frac{1}{k_2 q^2_{eq}} + \frac{1}{q^2_{eq}}\,t$	[59]
Intraparticular diffusion	$q_t = K_{id}{\cdot}t^{\frac{1}{2}} + C$	[60]

2.7. Adsorption Isotherm Studies

Equilibrium parameters and sulfur compound adsorption were tested using several isotherm models. This investigation was performed to evaluate the nature of the interactions that may exist between the obtained carbon and sulfur compounds. The Langmuir, Freundlich, Dubinin–Radushkevich, Tóth, and Sips models were used as isotherm models. Table 3 presents the linear forms of each model studied.

Table 3. Isotherm models.

Model	Equation	Linear Form	Reference
Langmuir	$q_e = \frac{q_m{\cdot}K_L{\cdot}C_e}{1+K_L{\cdot}C_e}$	$\frac{C_e}{q_e} = \frac{1}{q_m}{\cdot}C_e + \frac{1}{K_L{\cdot}q_m}$	[61]
Freundlich	$q_e = K_F{\cdot}C_e^{\frac{1}{n}}$	$\log(q_e) = \log(K_F) + \frac{1}{n}{\cdot}\log(C_e)$	[62]
Dubinin–Radushkevich	$\frac{q_e}{q_{mDR}} = \exp(-\beta\varepsilon^2)$	$\ln(q_e) = \ln(q_{mDR}) - (\frac{RT}{E})^2{\cdot}(\ln(\frac{C_S}{C_e})^2)$	[63]
Tóth	$\frac{q_e}{q_m} = \frac{K_L{\cdot}C_e}{[1+(K_L{\cdot}C_e)^n]^{1/n}}$	$(\frac{C_e}{q_e})^n = (\frac{1}{q_m{\cdot}K_L})^n + (\frac{1}{q_m})^n{\cdot}(C_e)^n$	[64]
Sips	$\frac{q_e}{q_m} = \frac{K_S{C_e}^n}{1+K_S{C_e}^n}$	$\frac{1}{q_e} = \frac{1}{q_m} + \frac{1}{K_L q_m {C_e}^n}$	[65]

3. Results and Discussion

3.1. Activated Carbon Characterization

Through calcination and HNO_3, H_2O_2, and KOH activation, the waste of cotton fibers was successfully transferred into activated carbon with different structures. Figure 3 shows the SEM images of the HNAC, HOAC, and KAC activated carbons. It can be seen that the chemical activation contributed to the formation of macroporosity. A hollow core can be observed throughout the length of the fiber, with a diameter of around 0.5–5.0 µM and an almost circular shape. The activated carbon has a highly porous structure, with a core diameter between approximately 0.5 and 5 µM (Figure 3b,d). This macroporosity may be related to the chemical destruction of lignin in the internal wall of the cotton fibers. The reference activated carbon (Figure 3a) presents macroporosity, while the morphology is characterized by the appearance of the core in the fiber, whose diameter depends on the activating agent. The largest diameter is obtained with the use of hydrogen peroxide as an activated reagent (Figure 3b). As shown in Figure 3b–d, the structure of the precursor (initially with a clean surface) is destroyed after each chemical treatment. Interestingly, the surface of the HOAC activated carbon changes obviously under the influence of chemical activation (compared with the other activated carbons).

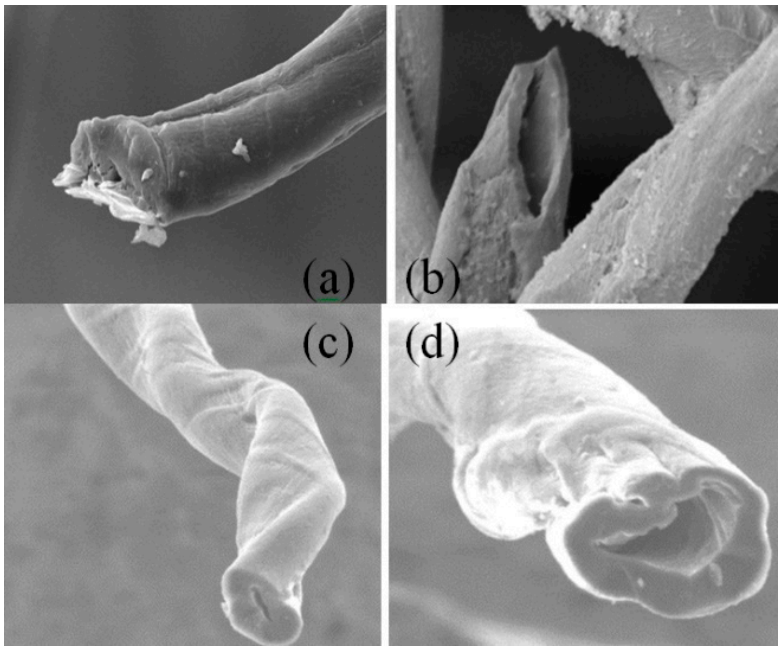

Figure 3. SEM images of activated carbon: (**a**) reference activated carbon, (**b**) HNAC, (**c**) HOAC, and (**d**) KAC.

The infrared spectra of the different activated carbons are shown in Figure 4. The FTIR spectrum of HOAC is shown in Figure 4c. It can be seen that the main spectral changes are restricted to between 1300 and 900 cm^{-1}. This indicates that the oxidation of the obtained char with the H_2O_2 solutions contributes to the increase in the number of OH surface groups. More precisely, these hydroxyl groups (OH) absorb radiation at 1195 cm^{-1}.

At 1300 cm^{-1}, there was a slight deviation in intensity. In fact, oxygen groups (C=O, CO_2^- or C=O) formed at very low concentrations. Moreover, for that reason, the oxidation state of the activated carbon surface did not improve because of the reaction with H_2O_2. Therefore, H_2O_2 was able to oxidize the material, and, hence, the surface chemistry of the AC was significantly altered

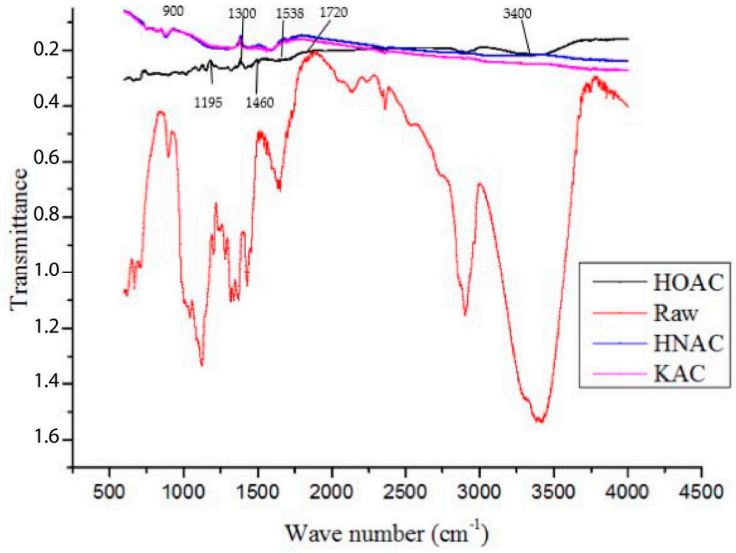

Figure 4. Infrared spectrum of different activated carbons: red line—reference activated carbons, blue line—HNAC, black line—HOAC, and purple line—KAC.

HNO_3 is a dehydrating agent that reduces the release of volatile matter and produces a high yield of carbon content in activated carbon.

According to Figure 4, we can conclude that there was a new modification of the FTIR spectrum of the HNAC sample and that new bands appeared. In fact, a new band at 1460 cm^{-1} was detected; this may be due to the vibrations of carboxyl groups (O–H). The increase in the intensity of the band at 1720 cm^{-1} can be assigned to the C=O stretching vibration. The band at 3400 cm^{-1}, due to the O–H stretching vibration, can be assigned to carboxyl acid groups. The existence of nitrate and nitro surface groups was confirmed by the appearance of new bands in the region of 1538 cm^{-1}. In conclusion, the chemical activation using HNO_3 fixed carboxyl groups and likely fixed nitro and nitrate groups. However, the activation using H_2O_2 and KOH probably fixed carboxyl, ketone, and ether groups. This was due to the nature of the activation using HNO_3, which can break the porous texture of the activated carbons compared with the other two oxidizing treatments. However, activation using H_2O_2 and KOH does not support the formation of ketone and ether groups.

The pore structure of the samples was determined using nitrogen adsorption at 77 K. The specific surface area was calculated using the Brunauer–Emmett–Teller equation. The micropore volume and surface area were calculated using a t-plot. According to Table 4, the maximal values of the pore volume size and specific surface area were identified in the chemical activation using H_2O_2. This was because oxidation treatment favors the dehydrogenation that was observed for this type of activation.

Table 4. Textural properties of the studied ACs, calculated using the data of N_2 adsorption isotherms.

	S_{BET} ($m^2 \cdot g^{-1}$)	V_t ($cm^3 \cdot g^{-1}$)	V_{DR} ($cm^3 \cdot g^{-1}$)	V_{MES} ($cm^3 \cdot g^{-1}$)
HOAC	1230	1.20	0.51	0.62
HNAC	842	1.03	0.48	0.59
KAC	915	1.08	0.49	0.60

As can be seen in the BJH pore size distribution, there was an obvious change in the distribution after carrying out the different chemical activation methods. The pore volume of HOAC was much larger than that of KAC and HNAC.

After the chemical activation, the BET surface areas of HOAC, HNAC, and KAC were 1230 $m^2 \cdot g^{-1}$, 840 $m^2 \cdot g^{-1}$, and 915 $m^2 \cdot g^{-1}$, respectively. Moreover, the mesopore

volume ratio of HOAC was higher than that of HNAC and KAC, providing more channels for ions to penetrate into the interior micropore surface area and leading to a good rate performance.

S_{BET} is the B_{ET} surface area calculated from the N_2 adsorption, V_t is the total pore volume of N_2, V_{DR} is the micropore volume determined using the Dubinin–Raduskevich equation, and V_{MES} is the volume of mesopores [63].

The lowest nitrogen uptake occurred for HNAC, which indicates a low specific surface area (840 $m^2 \cdot g^{-1}$). The profiles of the isotherms of HOAC, HNAC, and KAC were close to a type I isotherm with a H_4 type of loop (Figure 5). The branches of adsorption and desorption were nearly horizontal and parallel in the relative pressure range between 0.4 and 0.8.

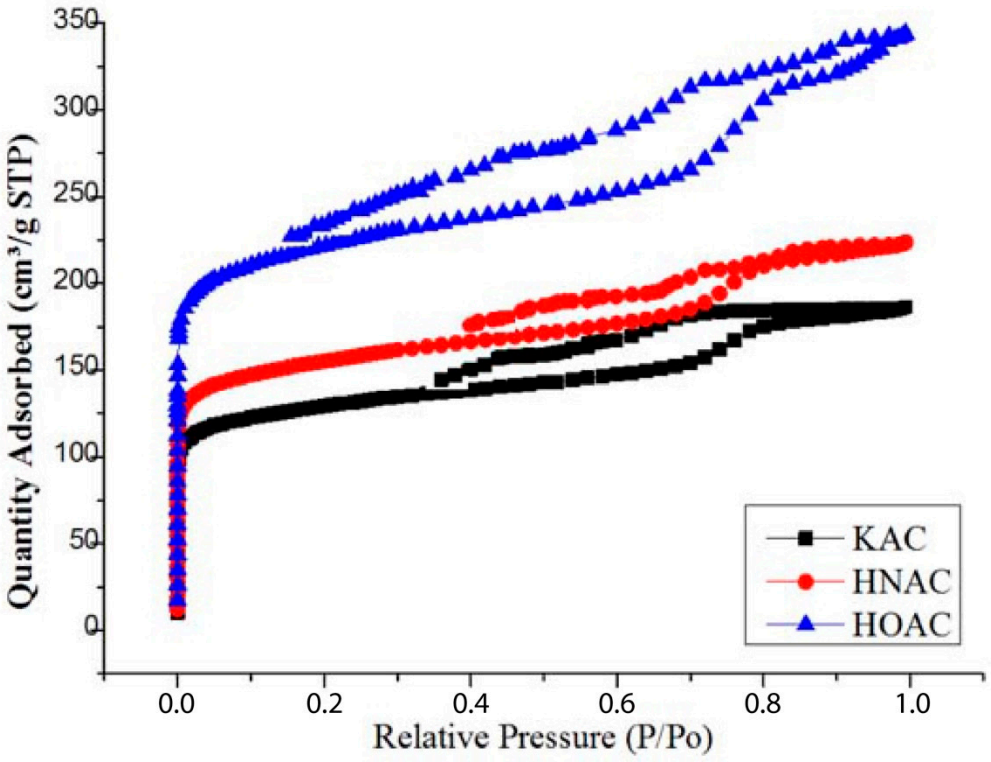

Figure 5. Effect of activated carbon dosage and wastewater flow on COD of reclaimed effluent.

The wider H_4 hysteresis loop of HOAC compared to that of HNAC and KAC indicates the domination of a mesoporous structure. However, this type of hysteresis corresponds to the existence of both micro- and meso-porous structures, which correspond to a large amount of N_2 being adsorbed in the entire relative pressure range. As is well-known, the effect of chemical activation is to open the pores of activated carbon wider in order to improve the chemical reagent efficacy.

As can be observed, nitric acid treatment can modify the porous structure of activated carbon, but the effect of peroxide oxidation is more pronounced. In the case of KOH activation, KOH diffused into the activated carbon and reacted both inside and outside simultaneously, leading to a developed pore structure.

To describe the adsorption isotherm of sulfur content by the synthesized activated carbons, mathematical models were investigated. In this experiment, the Freundlich and Langmuir models were used as the most common isotherms. The Freundlich parameters (k_f and n) were determined from the linear plot of log Q_e vs. log C_e. The Langmuir parameters (Q0 and b) were calculated from the plot of C_e/Q_e vs. C_e. All parameters are listed in Table 5.

Table 5. Summary of experimental design parameters.

Flow Rate (L/h)	Dosage Rate (mg/L)	COD_{HNAC} (mg/L)	COD_{HOAC} (mg/L)	COD_{KAC} (mg/L)
1	5	1585	1180	1870
1	10	644	485	778
1	15	252	183	304
1	25	60	4	68
2	5	1841	1375	2202
2	10	756	560	907
2	15	348	255	420
2	25	89	65	108
3	5	2105	1563	2515
3	10	912	674	1084
3	15	420	311	524
3	25	114	82	134
4	5	2340	1735	2811
4	10	1140	844	1352
4	15	530	375	621
4	25	135	105	163

The calculated RL values were between 0 and 1, which indicates favorable sulfur compound adsorption by the synthesized activated carbon.

As can be seen from the correlation coefficient (R^2), the Freundlich and Langmuir isotherms were able to describe the adsorption data obtained regarding the adsorption of the sulfur content onto the HOAC, HNAC, and KAC activated carbons. As summarized, the adsorption isotherms followed the Langmuir isotherm. This suggests that the homogenous surface and the adsorption follow the physisorption of monolayer adsorption patterns.

The better fit of the Langmuir model to the adsorption of the sulfur compounds onto both activated carbons shows that adsorption was found on the heterogeneous surface. Furthermore, there was an interaction between the adsorbed molecules and sulfur contents.

3.2. The Results of Fixed-Bed Adsorption

The adsorption bed column was installed as shown in Figure 1, and the refinery wastewater was allowed to flow under gravity. The diameter and the height of the bed column were 5.4 cm and 90 cm, respectively. The optimum adsorption conditions were determined for several parameters influencing the bed experiment, including the activated carbon dosage ratio and effluent flow. The experiments were designed using the response surface method. The results were analyzed using the analysis of variance method (ANOVA) to examine the effect of the parameters on the COD of the treated wastewater. Table 5 shows the 16 levels of the experimental design parameters and their results. For each of the 16 experiments, the COD was calculated. Figure 6 shows the effect of both activated carbon dosage and wastewater flow on the COD of the reclaimed effluent. For all samples of activated carbon at a high rate of wastewater flow, the COD was enhanced by an increase in the dosage mass. However, at a low flow rate, the COD was reduced. In summary, OHAC was the most effective adsorbent (compared with the HNAC and KAC activated carbons) in reducing the COD value of the refinery wastewater.

According to the contour plot (Figure 6), the COD value decreased with the flow rate of the effluent at a given saturation of each AC, and the decrease was nonlinear, particularly at low flow rates. This may be due to the combined effect of AC residence time. The lowest value of COD was obtained with the use of OHAC. This result was correlated with the activated carbon characteristics.

It can be concluded that the characteristic properties of activated carbon, such as the specific surface area, perfectly correlate with the decrease in COD. In fact, the highest value of the specific surface area (1230 $g \cdot m^{-2}$) was attributed to OHAC, which had the lowest value of COD.

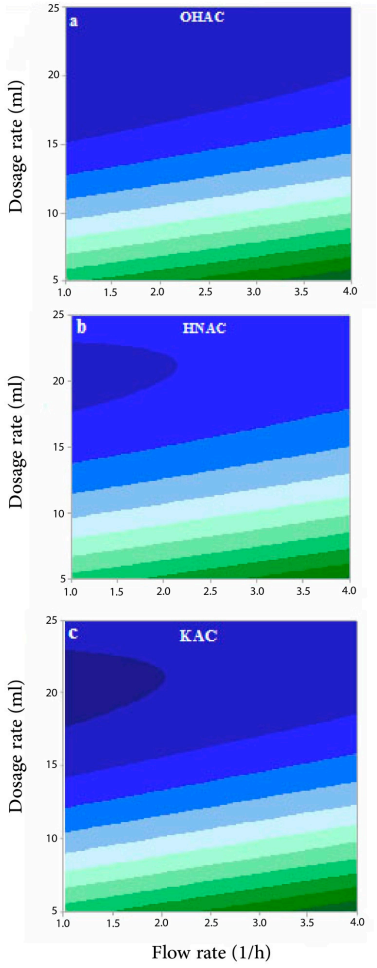

Figure 6. Contour plots of COD, (**a**) OHAC, (**b**) HNAC, and (**c**) KAC.

3.3. Adsorption Kinetics

Table 6 displays the kinetic parameters. To assess the relationship between the computed and experimental data, the correlation coefficient (R^2) was utilized. The pseudo-second-order model had the greatest R^2 value, as shown in Table 6. This indicates that the experimental data and the calculation for the pseudo-second-order kinetic model were well-correlated. As a result, the pseudo-second-order model can be considered a suitable kinetic model that fits the kinetic adsorption of sulfur compounds on HOAC activated carbon.

Table 6. Kinetic parameters of sulfur compound adsorption.

Kinetic Model	Model Parameters		R^2
Pseudo-first-order	q_e ($mg \cdot g^{-1}$) 120	K_1 (min^{-1}) 0.003	0.94
Pseudo-second-order	q_e ($mg \cdot g^{-1}$) 135	K_2 ($L \cdot mg^{-1} \cdot min^{-1}$) 11.10^{-4}	0.99
Intraparticular diffusion	K_{id} ($mg \cdot g^{-1} \cdot min^{-0.5}$) 11.20	C 0.13	0.91

The agreement between the experimental data and the model-predicted data was investigated by calculating correlation coefficients (R^2 values closer to 1 means a greater applicability of the model) and by observing the extent to which the experimental adsorption capacity is close to the theoretical value.

According to Table 6, there was an excellent connection between the experimental value and the pseudo-second-order calculated kinetic model. This result was determined due to the pseudo-second-order calculated kinetic model having the highest correlation coefficient R^2 value (0.99). Consequently, the pseudo-second-order model can be considered a suitable kinetic model that fits the kinetic adsorption of sulfur compounds on the HOAC. The electron exchange between the sulfur compounds and HOAC generated by the chemical adsorption resulted in a high valence liaison. As can be seen in Table 6, the pseudo-first-order and intraparticular diffusion models had low regression coefficient values ($R^2 < 0.94$). For the used kinetic model, a statistically significant difference was observed between the experimental and calculated adsorption capacities.

3.4. Modeling of Adsorption Isotherm

From the aqueous solutions, the equilibrium adsorption isotherms of the sulfur compounds were modeled and investigated on HOAC activated carbon. Five mathematical models were used in order to describe the experimental data of the adsorption isotherms. The main purpose of this work was to select the most suitable models that can describe the experimental results of the adsorption isotherms, determine the theoretical adsorption isotherm, and give the parameters. The initial goal was to develop a two-parameter equation in order to simulate the adsorption of sulfur compounds by HOAC. The experimental conditions were as follows: an initial sulfur concentration in a range between 5 and 300 mg·L^{-1}, agitation of 150 rpm, and a controlled temperature of 25 °C. For all isotherm models, the linear equation was investigated to determine its linear parameters with the use of experimental values of Q_e and C_e. The linear correlation coefficient (R^2) was used to evaluate the correlation between the theoretical and experimental values.

According to Table 7, we can conclude that the isotherm parameters were different. The Langmuir model has highest value of the correlation coefficient (R^2 = 0.98). This shows that the adsorption of the sulfur compounds on synthesized activated carbon follows the Langmuir isotherm. Both the Dubinin–Radushkevich and Tóth isotherms have the lowest correlation coefficient values (0.79 and 0.89, respectively), which suggests that these isotherms are not appropriate for this type of adsorption. However, the monolayer adsorption capacity obtained using the Langmuir isotherm is higher than that obtained using the other isotherm models. This indicates that all the active sites of the synthesized activated carbon (HOAC) are similar and that there is no interaction between the sulfur compounds.

Table 7. Linear isotherm parameters.

Model	*n*	K_L	q_m (mg·g^{-1})	R^2
Langmuir	0.84	0.02	168.4	0.98
Freundlich	0.84	0.01	17	0.96
Dubinin–Radushkevich	E0.16	-	-	0.79
Tóth	0.14	5.95×10^{-6}	115	0.89
Sips	0.79	0.01	241	0.97

4. Conclusions

In this study, solid waste from the spinning industry was investigated as a precursor of carbon materials. An ecofriendly activated carbon was successfully synthesized as an adsorbent of sulfur compounds in refinery wastewater. Kinetic and equilibrium data for the adsorption of sulfur compounds were obtained and fitted to Langmuir and pseudo-second-order models, respectively. The results show that introducing hydrogen peroxide, nitric acid, and potassium hydroxide can successfully increase the pore size distribution, pore volume, and surface area of carbon derived from cotton waste. In addition, HOAC (S_{BET} = 1230 m^2·g^{-1} and V_t = 1.20 cm^3·g^{-1}) had the best capacity to remove sulfur compounds compared to HNAC and KAC. It was found that, during fixed-bed adsorption, the

flow rate of effluent was the factor most effective at decreasing the COD of the refinery wastewater according to the responses and the ANOVA process.

The Langmuir model exhibited the best fit (R^2 = 0.98) for the sulfur compounds' adsorption, which implies that their adsorption onto the synthesized AC was homogeneous. The kinetic data were tested with pseudo-first-order, pseudo-second, and intraparticular diffusion equations. The pseudo-second-order equation showed the best description for the kinetic data (R^2 = 0.99), which means that this adsorption can be limited by the chemisorption process.

Several methods have been investigated for the treatment of refinery wastewater, including physical, chemical, and biological methods.

As a physical method, membrane bioreactors have been successfully used to remove pollutants from petroleum industry wastewater. However, membrane fouling is a major problem that can frequently occur. Moreover, this seriously affects the quality of the reclaimed water and the efficiency of the membrane. Its use has only been tested in a pilot test.

Electrochemical processes can also be utilized for the treatment of petroleum refinery wastewater. Their higher cost and lower efficiency also limit their industrial application.

The microbiological treatment of industrial refiner wastewater has also been investigated using several types of microorganisms. However, the use of a biological approach for refinery effluent treatment can cause serious problems due to the excessive production of sludge.

Many researchers have demonstrated that adsorption is a high-potential and cost-effective approach for the treatment of refinery wastewater. AC has previously been developed from biomass, such as date pits.

Most of these studies were conducted at the laboratory scale, with no focus on a specific application.

The main purpose of our work, realized with the collaboration of a big refinery company in Tunisia, was to synthesize activated carbon from low-quality cotton fiber spinning waste with and to use it to remove sulfur compounds from refinery wastewater. The results demonstrate the high efficiency of the obtained AC.

In comparison with other biomasses, cotton spinning waste can be used directly and does not need any selection or chemical treatment. This makes the management of this waste utilized directly as activated carbon easier.

Author Contributions: Conceptualization, B.W., M.K., I.B.H., R.A., Z.A., M.B.H., S.A., S.Z., M.T.K. and A.S.B.; Methodology, B.W., M.K., I.B.H. and A.S.B.; Validation, B.W., M.K., I.B.H. and A.S.B.; Data curation, B.W., M.K. and I.B.H.; Supervision, M.K. and M.B.H.; Visualization, M.K. and M.B.H.; Writing—original draft, M.K. and M.B.H.; Writing—review and editing, B.W., M.K., I.B.H., R.A., Z.A., M.B.H., S.A., S.Z., M.T.K. and A.S.B.; All authors have read and agreed to the published version of the manuscript.

Funding: This research received no external funding.

Institutional Review Board Statement: Not applicable.

Informed Consent Statement: Not applicable.

Data Availability Statement: This study did not report any data.

Conflicts of Interest: The authors declare no conflict of interest.

References

1. Speight, J.G. *Handbook of Petroleum Refining*; Taylor & Francis G: Boca Raton, FL, USA, 2017. Available online: https://www.crcpress.com/Handbook-of-Petroleum-Refining/Speight/p/book/9781466591608 (accessed on 20 July 2022).
2. Panizza, M. Fine Chemical Industry, Pulp and Paper Industry, Petrochemical Industry and Pharmaceutical Industry. In *Electrochemical Water and Wastewater Treatment*; Elsevier Inc.: Genoa, Italy, 2018; pp. 335–364. Available online: https://www.sciencedirect.com/science/article/pii/B9780128131602000134 (accessed on 15 July 2022).

3. Noor Ul Huda, K.; Shimizu, K.; Gong, X.; Takagi, S. Numerical investigation of COD reduction in compact bioreactor with bubble plumes. *Chem. Eng. Sci.* **2018**, *185*, 1–17. [CrossRef]
4. Abdulredha, M.M.; Aslina, H.S.; Luqman, C.A. Overview on petroleum emulsions, formation, influence and demulsification treatment techniques. *Arab. J. Chem.* **2020**, *13*, 3403–3428. [CrossRef]
5. De Oliveira, C.P.M.; Viana, M.M.; Amaral, M.C.S. Coupling photocatalytic degradation using a green TiO_2 catalyst to membrane bioreactor for petroleum refinery wastewater reclamation. *J. Water Process Eng.* **2020**, *34*, 101093. [CrossRef]
6. Mohammadi, L.; Rahdar, A.; Bazrafshan, E.; Dahmardeh, H.; Susan, M.; Hasan, A.B.; Kyzas, G.Z. Petroleum Hydrocarbon Removal from Wastewaters: A Review. *Processes* **2020**, *8*, 447. [CrossRef]
7. Coppock, R.W.; Christian, R.G. Chapter 50—Petroleum. In *Veterinary Toxicology*, 3rd ed.; Gupta, R.C., Ed.; Academic Press: Cambridge, MA, USA, 2018; pp. 659–673. Available online: http://www.sciencedirect.com/science/article/pii/B9780128114100000507 (accessed on 20 July 2022).
8. Han, Y.; Zhang, Y.; Xu, C.; Hsu, C.S. Molecular characterization of sulfur-containing compounds in petroleum. *Fuel* **2018**, *221*, 144–158. [CrossRef]
9. Pérez, R.M.; Cabrera, G.; Gómez, J.M.; Ábalos, A.; Cantero, D. Combined strategy for the precipitation of heavy metals and biodegradation of petroleum in industrial wastewaters. *J. Hazard. Mater.* **2010**, *182*, 896–902. [CrossRef] [PubMed]
10. Rahman, M.M.; Al-Malack, M.H. Performance of a crossflow membrane bioreactor (CF–MBR) when treating refinery wastewater. *Desalination* **2006**, *191*, 16–26. [CrossRef]
11. Razavi, S.M.R.; Miri, T. A real petroleum refinery wastewater treatment using hollow fiber membrane bioreactor (HF-MBR). *J. Water Process Eng.* **2015**, *8*, 136–141. [CrossRef]
12. Abass, O.K.; Fang, F.; Zhuo, M.; Zhang, K. Integrated interrogation of causes of membrane fouling in a pilot-scale anoxic-oxic membrane bioreactor treating oil refinery wastewater. *Sci. Total Environ.* **2018**, *642*, 77–89. [CrossRef]
13. Munirasu, S.; Haija, M.A.; Banat, F. Use of membrane technology for oil field and refinery produced water treatment—A review. *Process Saf. Environ. Prot.* **2016**, *100*, 183–202. [CrossRef]
14. Sari Erkan, H.; Bakaraki Turan, N.; Önkal Engin, G. Chapter Five—Membrane Bioreactors for Wastewater Treatment. In *Comprehensive Analytical Chemistry*; Chormey, D.S., Bakırdere, S., Turan, N.B., Engin, G.Ö., Eds.; Elsevier: Amsterdam, The Netherlands, 2018; Volume 81, pp. 151–200. Available online: http://www.sciencedirect.com/science/article/pii/S0166526X18300035 (accessed on 20 July 2022).
15. Yan, L.; Ma, H.; Wang, B.; Wang, Y.; Chen, Y. Electrochemical treatment of petroleum refinery wastewater with three-dimensional multi-phase electrode. *Desalination* **2011**, *276*, 397–402. [CrossRef]
16. El-Naas, M.H.; Al-Zuhair, S.; Al-Lobaney, A.; Makhlouf, S. Assessment of electrocoagulation for the treatment of petroleum refinery wastewater. *J. Environ. Manag.* **2009**, *91*, 180–185. [CrossRef] [PubMed]
17. Yan, L.; Wang, Y.; Li, J.; Ma, H.; Liu, H.; Li, T.; Zhang, Y. Comparative study of different electrochemical methods for petroleum refinery wastewater treatment. *Desalination* **2014**, *341*, 87–93. [CrossRef]
18. El-Naas, M.H.; Alhaija, M.A.; Al-Zuhair, S. Evaluation of a three-step process for the treatment of petroleum refinery wastewater. *J. Environ. Chem. Eng.* **2014**, *2*, 56–62. [CrossRef]
19. Zhu, X.; Ni, J.; Xing, X.; Li, H.; Jiang, Y. Synergies between electrochemical oxidation and activated carbon adsorption in three-dimensional boron-doped diamond anode system. *Electrochim. Acta* **2011**, *56*, 1270–1274. [CrossRef]
20. Krstić, V.; Urošević, T.; Pešovski, B. A review on adsorbents for treatment of water and wastewaters containing copper ions. *Chem. Eng. Sci.* **2018**, *192*, 273–287. [CrossRef]
21. Li, B.; Sun, K.; Guo, Y.; Tian, J.; Xue, Y.; Sun, D. Adsorption kinetics of phenol from water on Fe/AC. *Fuel* **2013**, *110*, 99–106. [CrossRef]
22. Ebrahimi, M.; Kazemi, H.; Mirbagheri, S.A.; Rockaway, T.D. An optimized biological approach for treatment of petroleum refinery wastewater. *J. Environ. Chem. Eng.* **2016**, *4*, 3401–3408. [CrossRef]
23. Wang, Y.; Wang, Q.; Li, M.; Yang, Y.; He, W.; Yan, G.; Guo, S. An alternative anaerobic treatment process for treatment of heavy oil refinery wastewater containing polar organics. *Biochem. Eng. J.* **2016**, *105*, 44–51. [CrossRef]
24. Fakhru'l-Razi, A.; Pendashteh, A.; Abdullah, L.C.; Biak, D.R.A.; Madaeni, S.S.; Abidin, Z.Z. Review of technologies for oil and gas produced water treatment. *J. Hazard. Mater.* **2009**, *170*, 530–551. [CrossRef]
25. Ma, F.; Guo, J.; Zhao, L.; Chang, C.; Cui, D. Application of bioaugmentation to improve the activated sludge system into the contact oxidation system treating petrochemical wastewater. *Bioresour. Technol.* **2009**, *100*, 597–602. [CrossRef] [PubMed]
26. Hayat, S.; Ahmad, I.; Azam, Z.M.; Ahmad, A.; Inam, A. Effect of long-term application of oil refinery wastewater on soil health with special reference to microbiological characteristics. *Bioresour. Technol.* **2002**, *84*, 159–163. [CrossRef]
27. Louhıchı, G.; Bousselmı, L.; Ghrabı, A.; Khounı, I. Process optimization via response surface methodology in the physico-chemical treatment of vegetable oil refinery wastewater. *Environ. Sci. Pollut. Res.* **2018**, *26*, 18993–19011. [CrossRef]
28. El-Naas, M.H.; Alhaija, M.A.; Al-Zuhair, S. Evaluation of an activated carbon packed bed for the adsorption of phenols from petroleum refinery wastewater. *Environ. Sci. Pollut. Res.* **2017**, *24*, 7511–7520. [CrossRef]
29. Alvarez, J.; Amutio, M.; Lopez, G.; Bilbao, J.; Olazar, M. Fast co-pyrolysis of sewage sludge and lignocellulosic biomass in a conical spouted bed reactor. *Fuel* **2015**, *159*, 810–818. [CrossRef]
30. Dehghan, R.; Anbia, M. Zeolites for adsorptive desulfurization from fuels: A review. *Fuel Process. Technol.* **2017**, *167*, 99–116. [CrossRef]

31. Moradi, M.; Karimzadeh, R.; Moosavi, E.S. Modified and ion exchanged clinoptilolite for the adsorptive removal of sulfur compounds in a model fuel: New adsorbents for desulfurization. *Fuel* **2018**, *217*, 467–477. [CrossRef]
32. El-Naas, M.H.; Al-Zuhair, S.; Alhaija, M.A. Removal of phenol from petroleum refinery wastewater through adsorption on date-pit activated carbon. *Chem. Eng. J.* **2010**, *162*, 997–1005. [CrossRef]
33. Qingxuan, Z. COD Removal in Refinery Wastewater through Adsorption on Activated Petroleum Coke. In Proceedings of the 2011 International Conference on Computer Distributed Control and Intelligent Environmental Monitoring, Changsha, China, 19–20 February 2011; pp. 1093–1096. [CrossRef]
34. Garole, D.J.; Choudhary, B.C.; Paul, D.; Borse, A.U. Sorption and recovery of platinum from simulated spent catalyst solution and refinery wastewater using chemically modified biomass as a novel sorbent. *Environ. Sci. Pollut. Res. Int.* **2018**, *25*, 10911–10925. [CrossRef]
35. Mohammad, Y.S.; Shaibu-Imodagbe, E.M.; Igboro, S.B.; Giwa, A.; Okuofu, C.A. Adsorption of Phenol from Refinery Wastewater Using Rice Husk Activated Carbon. *Iran. J. Energy Environ.* **2014**, *5*, 393–399.
36. Mushrif, S.H.; Vasudevan, V.; Krishnamurthy, C.B.; Venkatesh, B. Multiscale molecular modeling can be an effective tool to aid the development of biomass conversion technology: A perspective. *Chem. Eng. Sci.* **2015**, *121*, 217–235. [CrossRef]
37. Rout, P.K.; Nannaware, A.D.; Prakash, O.; Kalra, A.; Rajasekharan, R. Synthesis of hydroxymethylfurfural from cellulose using green processes: A promising biochemical and biofuel feedstock. *Chem. Eng. Sci.* **2016**, *142*, 318–346. [CrossRef]
38. El-Naas, M.H.; Al-Zuhair, S.; Alhaija, M.A. Reduction of COD in refinery wastewater through adsorption on date-pit activated carbon. *J. Hazard. Mater.* **2010**, *173*, 750–757. [CrossRef] [PubMed]
39. Juanga-Labayen, J.P.; Labayen, I.V.; Yuan, Q. A Review on Textile Recycling Practices and Challenges. *Textiles* **2022**, *2*, 174–188. [CrossRef]
40. Claudio, L. Waste couture: Environmental Impact of the Clothing Industry. *Environ. Health Perspect.* **2007**, *115*, A448–A454. [CrossRef]
41. Hasanzadeh, E.; Mirmohamadsadeghi, S.; Karimi, K. Enhancing energy production from waste textile by hydrolysis of synthetic parts. *Fuel* **2018**, *218*, 41–48. [CrossRef]
42. Shen, B.; Chen, J.; Yue, S.; Li, G. A comparative study of modified cotton biochar and activated carbon based catalysts in low temperature SCR. *Fuel* **2015**, *156*, 47–53. [CrossRef]
43. Kanan, M.; Wannassi, B.; Barham, A.S.; Ben Hassen, M.; Assaf, R. The Quality of Blended Cotton and Denim Waste Fibres: The Effect of Blend Ratio and Waste Category. *Fibers* **2022**, *10*, 76. [CrossRef]
44. Halimi, M.T.; Hassen, M.B.; Azzouz, B.; Sakli, F. Effect of Cotton Waste and Spinning Parameters on Rotor Yarn Quality. *J. Text. Inst.* **2007**, *98*, 437–442. [CrossRef]
45. Halimi, M.T.; Hassen, M.B.; Sakli, F. Cotton Waste Recycling: Quantitative and Qualitative Assessment. *Resour. Conserv. Recycl.* **2008**, *52*, 785–791. [CrossRef]
46. Wanassi, B.; Azzouz, B.; Hassen, M.B. Value-Added Waste Cotton Yarn: Optimization of Recycling Process and Spinning of Reclaimed Fibers. *Ind. Crops Prod.* **2016**, *87*, 27–32. [CrossRef]
47. Abidi, H.; Rana, S.; Chaouch, W.; Azouz, B.; Aissa, I.B.; Hassen, M.B.; Fangueiro, R. Accelerated Weathering of Textile Waste Nonwovens Used as Sustainable Agricultural Mulching. *J. Ind. Text.* **2019**, *50*, 1079–1110. [CrossRef]
48. USEPA (United States Environmental Protection Agency). Facts and Figures about Materials, Waste and Recycling 2021. Textiles: Material-Specific Data, Summary Table and Graph. Available online: https://www.epa.gov/facts-and-figures-about-materialswaste-and-recycling/textiles-material-specific-data#TextilesTableandGraph (accessed on 15 January 2022).
49. Triki, A.; Wanassi, B.; Hassen, M.; Arous, M.; Kallel, A. Dieletric Analysis of Unsaturated Polyester Composite Reinforced with Recycled Cotton Textile Residues. *Int. J. Appl. Res. Text.* **2019**, 44–50. Available online: http://atctex.org/ijartex/index.php?mayor=magazine&id=50 (accessed on 22 July 2022).
50. Temmink, R.; Baghaei, B.; Skrifvars, M. Development of Biocomposites from Denim Waste and Thermoset Bio-Resins for Structural Applications. *Compos. Part A Appl. Sci. Manuf.* **2018**, *106*, 59–69. [CrossRef]
51. Zhao, Q.; Ye, Z.; Zheng, J. Preparation and characterization of activated carbon fiber (ACF) from cotton woven waste. *Appl. Surface Sci.* **2014**, *299*, 86–91. [CrossRef]
52. Sartova, K.; Omurzak, E.; Kambarova, G.; Dzhumaev, I.; Borkoev, B.; Abdullaeva, Z. Activated carbon obtained from the cotton processing wastes. *Diam. Relat. Mater.* **2019**, *91*, 90–97. [CrossRef]
53. Wanassi, B.; Hariz, I.B.; Ghimbeu, C.M.; Vaulot, C.; Hassen, M.B.; Jeguirim, M. Carbonaceous adsorbents derived from textile cotton waste for the removal of Alizarin S dye from aqueous effluent: Kinetic and equilibrium studies. *Environ. Sci. Pollut. Res.* **2017**, *24*, 10041–10055. [CrossRef]
54. Xu, Z.; Zhang, T.; Yuan, Z.; Zhang, D.; Sun, Z.; Huang, Y.X.; Chen, W.; Tian, D.; Deng, H.; Zhou, Y. Fabrication of cotton textile waste-based magnetic activated carbon using FeCl3 activation by the Box-Behnken design: Optimization and characteristics. *RSC Adv.* **2018**, *8*, 38081–38090. [CrossRef]
55. Xu, Z.; Zhou, Y.; Sun, Z.; Zhang, D.; Huang, Y.; Gu, S.; Chen, W. Understanding reactions and pore-forming mechanisms between waste cotton woven and FeCl3 during the synthesis of magnetic activated carbon. *Chemosphere* **2020**, *241*, 125120. [CrossRef]
56. Lu, J.; Wang, Z.; Ma, X.; Tang, Q.; Li, Y. Modeling of the electrocoagulation process: A study on the mass transfer of electrolysis and hydrolysis products. *Chem. Eng. Sci.* **2017**, *165*, 165–176. [CrossRef]

57. El-Naas, M.H.; Surkatti, R.; Al-Zuhair, S. Petroleum refinery wastewater treatment: A pilot scale study. *J. Water Process Eng.* **2016**, *14*, 71–76. [CrossRef]
58. Lagergren, S. About the Theory of so Called Adsorption of Soluble Substances. *K. Sven. Vet. Akad. Handl.* **1998**, *24*, 1–39.
59. Ho, Y.S.; Mckkay, G. Pseudo-second order model for sorption processes. *Process Biochem.* **1999**, *34*, 451–465. [CrossRef]
60. Kumar, D.B.; Smail, K. Étude cinétique et thermodynamique de l'adsorption d'un colorant basique sur la sciure de Bois. *Revue des Sciences de l'Eau J. Water Sci.* **2011**, *24*, 131–144.
61. Langmuir, I. The Adsorption of Gases on Plane Surfaces. *J. Am. Chem. Soc.* **1918**, *40*, 1361–1403. [CrossRef]
62. Freundlich, H. Adsorption in Solution. *Z. Phys. Chem.* **1906**, *57*, 384–470.
63. Dubinin, M.M. The Potential Theory of Adsorption of Gases and Vapors for Adsorbents with Energetically Nonuniform Surfaces. *Chem. Rev.* **1960**, *60*, 235–241. [CrossRef]
64. Gimbert, F.; Morin-Crini, N.; Renault, F.; Badot, P.-M.; Crini, G. Adsorption isotherm models for dye removal by cationized starch-based material in a single component system: Error analysis. *J. Hazard. Mater.* **2008**, *157*, 34–46. [CrossRef]
65. Sips, R. On the Structure of a Catalyst Surface. *J. Chem. Phys.* **1948**, *16*, 490–495. [CrossRef]